EXPLAINING HIGH PERMEABILITY ON LOCALISED FAULT ZONES THROUGH THMC FEEDBACKS – A SOULTZ-SOUS-FORETS INSPIRED APPROACH

Rebecca Tung[1], Thomas Poulet[2,3], Max Peters[4], Manolis Veveakis[5], and Klaus Regenauer-Lieb[3]

[1] Department of Exploration Geophysics, Curtin University, Australia

[2] CSIRO Mineral Resources, Kensington WA, Australia

[3] School of Minerals and Energy Resources, UNSW Sydney, Australia

[4] Karlsruhe Institute of Technology, Germany

[5] Department of Civil and Environmental Engineering, Duke University, Durham, North Carolina, USA

rebecca.tung@postgrad.curtin.edu.au

Keywords: *THMC couplings, fault zone permeability, hydrothermal convection, chemical reactions, mechanical instabilities.*

ABSTRACT

Geothermal systems portray a rich style of coupled Thermal, Hydraulic, Mechanical, and Chemical (THMC) processes that underpin the heat transfer in a variety of geothermal manifestations. A particularly interesting phenomenon is the fault-bounded transfer of hot fluid in settings such as the Soultz-sous-Forêts graben-hosted geothermal resource. This data-rich environment allows detailed insights into the processes and serves as a benchmark for numerical modelling of such systems. Conceptual models can be devised that duplicate the anomalous thermal gradient by assigning arbitrarily high permeabilities to fault zones. However, the models do not match geological/geophysical observables of these fault zones, which in particular have a much lower permeability than the best-fit values of the models. Here we show - in a systematic numerical analysis - the potential contribution of TH, THM, and THMC feedback processes that can reconcile geophysical/geological observations with the observed heat transfer. The classical TH models without additional feedbacks require unrealistically high permeabilities ($10^{-14} - 10^{-15}$m^2), and too wide fault zones. THM solutions require extreme deformation rates ($10-^{13}$s^{-1}) to match the heat profile with the observed permeability. We suggest that a THMC solution could reproduce the observations with realistic values of permeability (10^{-16}m^2), fault zone widths ($\ll$ 100m), and strain rates (10^{-16}s^{-1}). Our analysis shows that fault zone permeability can be a dynamic process significantly enhanced by chemical reactions. In a fully-coupled system, these reactions are oscillating at relatively short timescales and allows us to couple geodynamic timescales with shorter engineering timescales. The implications of this analysis also have bearings on borehole stability and reservoir integrity, and may open new pathways for reservoir stimulation.

1. GEOLOGICAL SETTING AND GEOTHERMAL OBSERVATIONS

The Soultz-sous-Forêts geothermal resource is located in the Rhine Graben in Europe, and represents the target of the European Hot Dry Rock project. The Graben was formed as a result of alpine orogeny in the European Cenozoic rift system (Ziegler, 1992). Mesozoic and Cenozoic sediments overlay the top 1400m of a Paleozoic granitic basement, which extends down to 5000m (Pribnow and Schellschmidt, 2000). Prominent large-scale north-south striking faults are identified to originate in the granitic basement and extend up through the sedimentary cover (Rousset et al., 1993). The large quantity of temperature data, fracture networks, seismic activity, and chemical alteration history obtained from geophysical data and borehole logs indicate that coupled thermo-hydro-mechanical-chemical (THMC) processes are present in such a setting. Field evidence of these processes have been thoroughly analysed and a brief summary is presented below.

1.1 Evidence of Mechanical Deformation

Since the formation of the Rhine Graben, various rift segments have experienced changes in the stress field and still remain tectonically active today (Ziegler, 1992). Recent seismic data indicate that vertical movement in the graben is attributed to ongoing sub-crustal upwelling, supported by the presence of geothermal anomalies, seismic activity, and recent neotectonic movements (Buchmann and Connolly, 2007). Active faults appear to creep at a continuous rate without any major seismic activity (Illies and Greiner, 1978), and reactivation of prior fault margins could have been triggered by four major stress field re-orientations from the Eocene age to the present (Bergerat, 1987; Larroque and Laurent, 1988). Albeit the many stress reorientations since the creation of the graben, the southern Rhine Graben area is currently characterised by normal and strike-slip faulting movements (Plenefisch and Bonjer, 1997).

Various scales of deformation are present at Soultz, ranging from large scale faults (e.g. Soultz and Kutzenhausen) to small scale fractures observed in borehole imaging techniques. The aperture and orientations of fracture clusters found in boreholes indicate complex deformation history and stress fields (Sausse et al., 2010). Although major large-scale faults play a role in enhancing heat and fluid flow in the Graben, of particular interest are the small-scale fractures in the granitic basement. Structural and geometrical data of these fractures obtained from well log analyses, microseismicity interpretation and hydraulic well stimulation (Dezayes et al., 2010; Sausse et al., 2010) confirm the presence of fluid flow circulating within faults and fracture zones, interpreted from a temperature profile obtained from well GPK2 (Figure 8 of Genter et al. (2010)). Due to the focus on hydrothermal flow, the terms ’fracture zone’ and ’fault’ are often used interchangeably. This points to the need to investigate the role of faults on hydrothermal convection.

1.2 Evidence of Hydrothermal Convection

At Soultz, prominent hot and cold upwellings are found at both regional and local scales. Homogeneously paired hot-cold patterns at depths of 800m are approximately 20km apart on a regional scale (Pribnow and Schellschmidt, 2000), but exhibit different characteristics on a local scale. A non-homonegeous distribution of convective up- and down-wellings are found at a scale of a few kilometres (see Figure 1), where hot upwellings are seen to concentrate around fault zones (Bächler et al., 2003).

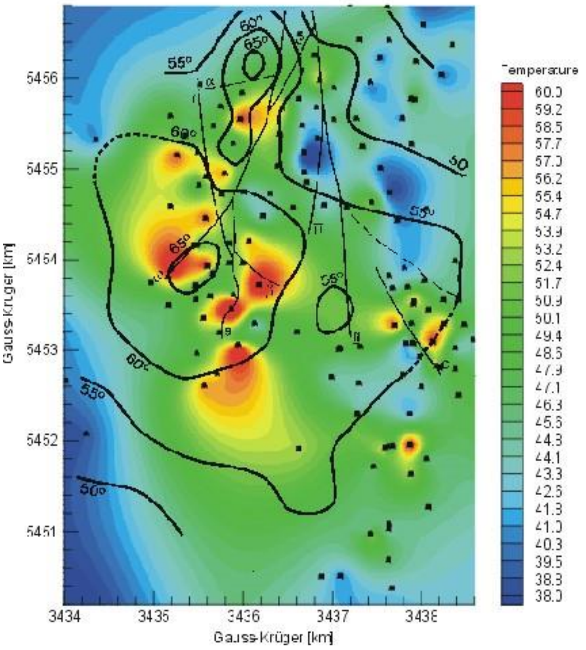

Figure 1: Local temperature scale of Soultz; 1km scale, 500m depth. (Coloured version from (Bächler et al., 2003), personal communication.)

Temperature information obtained from well data (GPK2) confirms the presence of hydrothermal convection and asserts the influential role of faults acting as pathways for heat and fluid transport. Heated fluid travels upwards through sub-vertical fracture networks and is circulated in the sediments (Pribnow and Schellschmidt, 2000). In Figure 2, temperature gradients are approximated at three instances along the profile. The highest branch (closest to the surface) has the highest thermal gradient, which has been interpreted as the diffusion (conduction) of heat from a high convective heat source below (Vidal et al., 2015). The middle branch has an extremely low thermal gradient, implying the vertical flow of fluid up to the sediments, and the lower branch has a gradient similar to the normal geothermal gradient. The backflow of temperature located at depths of approximately 2100m and 3500m are thermal signature of fault zones (Vidal et al., 2015). The change in geothermal gradient at approximately 1400m depth could most probably be attributed to the contrast in permeability and thermal conductivity of the sediment-basement interface, where a highly altered granitic basement is overlaid by clay sediments (Pribnow and Clauser, 2000; Pribnow and Schellschmidt, 2000).

Of particular interest is the fault located at 3500m depth. It is located at the interface between two changing geothermal gradients, without any major changes in geological units or material properties (Hooijkaas et al., 2006). It is investigated whether this fault could be the key parameter that governs the existence of convection.

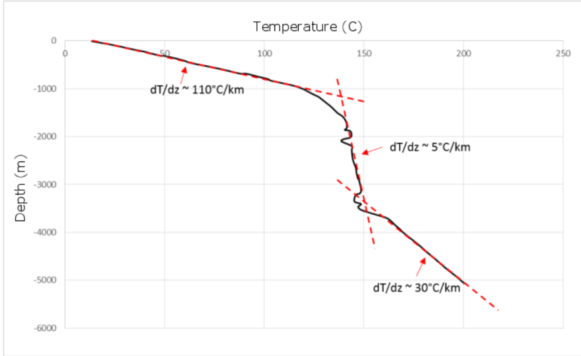

Figure 2: Temperature profile obtained from well GPK2, data source from Genter et al. (2010).

1.3 Convection in the Upper Reservoir

Vidal et al. (2015) proposes a conceptual model of a local convective cell with a sub-vertical fracture network controlling fluid circulation, especially between 1400m and 3500m depth in the granite, termed as the 'upper reservoir'. This corresponds to the upflow of hot fluid through the granite and its diffusion into the sediments, seen in Figure 2. The lithology of these upper-lying sediments, sediment-granite interface at 1400m, and granitic host rock have been studied extensively through petrographical sections of lithology, fracture orientation, aperture, and hydrothermal alterations (e.g. Dezayes et al., 1995; Hooijkaas et al., 2006; Sausse et al., 2006; Vidal et al., 2015, 2017). Additionally, considerable information is present and various models have been analysed to understand physical processes occurring in the lower reservoir (Dezayes et al., 2004, 2010; Ledésert et al., 2010; Sausse et al., 2010). The interface between the upper and lower reservoir, however, has not yet been fully understood, particularly the fault at 3500m depth.

The fracture conditions at this interface documented by Sausse et al. (2010) and Dezayes et al. (2010) indicate a contrast in hydrothermally altered granite, where the upper boundary predominantly consists of abundant vein alterations while biotite-amphibole rich granite dominates the lower boundary.

2. COMPILATION OF PREVIOUS MODELS

Extensive studies have investigated the behaviour of convection on both regional and local scales using numerical models (Clauser and Villinger, 1990; Le Carlier et al., 1994; Benderitter and Elsass, 1996; Kohl et al., 2000; Bächler et al., 2003; Pribnow and Schellschmidt, 2000). In these studies, there have been two main approaches: a homogeneous approach in which convection is dependent on the average permeability of geological units (e.g. Le Carlier et al., 1994; Magnenet et al., 2014), and a fractured approach in which fault permeability is taken into account (e.g. Bächler et al., 2003). This section presents an overview and highlights the results of the two approaches.

2.1 Homogeneous vs. Fractured Approaches

Numerical studies have been performed to understand the effect of convection in large-scale geometries, where homogeneous (i.e. single) permeabilities were assigned to all strata to represent various geological lithologies. Le Carlier et al. (1994) investigated the permeability required for convection to occur in the Soultz reservoir was in the order of $k=10^{-14}m^2$, with the reservoir dimensions measuring approximately 60km in length and 5km in depth.

Also at Soultz, Magnenet et al. (2014) examined a steady state solution of a convective system from a simplified two-dimensional numerical model, with dimensions 10km in length and 5.3km in depth. Focusing on the rich rheologies of rocks and brine, the model assumed homogenised horizontal layers. For natural convection to occur in this reservoir, the minimum permeability required was also in the order of $k=10^{-14}m^2$, where a periodic pair of convection cells measured approximately 2.6km in width. Whilst this approach captures the essential mode of heat transfer in the Rhine Graben on a regional scale, it is at odds with the observation on the smaller scales where localised upwellings and downwellings can be identified at much shorter wavelengths (Bächler et al., 2003). This is particularly obvious around fault zones and their intersections (Figure 1).

In the fractured modelling approach, numerical models considering fault geometry and material properties were included in order to observe its effects on convection in the reservoir. The work of Bächler et al. (2003) highlights the importance of fault permeability at Soultz, particularly in sub-vertical faults which facilitate natural up- and down-welling flow in the Rhine Graben. In this study, convection was found to occur at values of $k=4.8\times10^{-14}m^2$ for a fault width of 200m. Geophysical evidence from gravity data also support fractures controlling fluid flow (Baillieux et al., 2014), and large-scale temperature anomalies can be attributed to the intersection of several highly permeable sub-vertical faults, notably the Kutzenhausen and Soultz Fault Systems, for instance.

2.2. Motivation and aim for this study

Figure 2 indicates temperature deviations at depths of approximately 3242m and 3514m from the GPK2 wellbore. These correspond to major fracture zones which, interestingly, exhibited low permeability during low-pressure hydraulic tests (Jung et al., 1995). Information from the GPK1 wellbore identifies a fracture zone at 3492m which was a dominant permeable structure (Evans et al., 2005). Although this fracture zone is not recorded in GPK2 logs, its location at the intersection of changing temperature gradients is notable.

The aim for this study is to investigate how this fracture zone may or may not control the character of convection in the upper-lying strata.

3. MATERIALS AND METHODS

The numerical tool used in this study is REDBACK (Poulet et al., 2017), following the workflow described in Tung (2018). This study investigates the physical processes responsible for the convection pattern observed, trying to first explain it from a simple hydrothermal perspective, and with the consideration of more processes as required. All equations solved (i.e. mass and energy balance) are detailed in Tung et al. (2017).

3.1 Model Parameterization

In order to investigate the effects of THM couplings without the additional complexity and drivers from the geometry and boundary conditions of the real geological scenario, this modelling study is based on a representative but simplified convection cell pinned by sub-vertical fracture zones. As such, the geological drivers are parameterised by the homogeneous material properties of these fracture zones, mainly by their dimensionless Gruntfest (Gr) and Lewis (Le) numbers characterising respectively the amount of shear heating and permeability – see Tung et al. (2017). The sub-vertical faults in the model are assumed to be made up of multi-scale fracture networks which connect the overlying sediments and permeate the granitic basement rock. For simplicity, a representative 2D vertical cross-section shown in Figure 3 is taken through the faults, which are assumed to extend infinitely in the third dimension so any end-effects of the faults are ignored. In order to close the fault network, these sub-vertical faults are assumed to be connected horizontally at depths of 1400m and 3500m, respectively representing the interface between overlying sediment and granitic rock (1400m), and the fault of interest (3492m). In addition, the fracture network is homogenised by an effective permeability which is assumed to be isotropic.

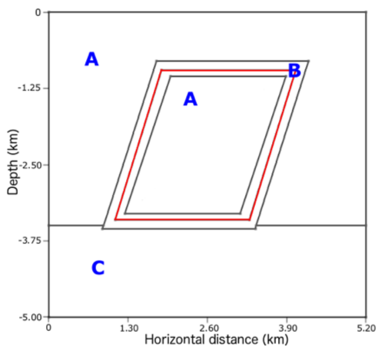

Figure 3: Conceptual mesh geometry used in this study. Three rock lithologies represented in the model are: the granitic host rock (A), ~60º dipping fault network (B) with the centre of the fault zone marked in red, and granitic basement (C).

Three rock lithologies are represented in the model; the combined granitic host rock and overlying sediments (type A in Fig. 3), the fracture network (type B), and the granitic basement (type C). In order to understand the role of the fracture network affecting fluid flow processes, the study focuses on a conceptualised zone of interest of 5km depth, including the representative convection cell described above.

Table of Parameters for matching the Temperature Profile of GPK2			
		Real Values	Dimensionless Values
Geometry	Height	5000 (m)	5
	Length	5200 (m)	5.2
	Fault width	370 (m)	–
Boundary Conditions	Temperature top	293 (K)	0.0
	Temperature bottom	473 (K)	1.0
	Pressure top	1E+05 (Pa)	2.04E-03
	Gravity	9.8 ($m \cdot s^{-1}$)	-1.03
Fluid Properties	Thermal expansion coefficient	7E-05 (K^{-1})	1.26E-02
	Compressibility	4E-10 (Pa^{-1})	1.96E-02
	Viscosity	1.2E-04 ($Pa \cdot s$)	–
	Density	1000 ($kg \cdot m^{-3}$)	1.0
	Specific heat	1000 ($J \cdot kg^{-1} \cdot K^{-1}$)	–
	Permeability (A)	1.84E-17 (m^2)	1E-03
	Permeability (B)	2.30E-15 (m^2)	1e-05
	Permeability (C)	3.68E-16 (m^2)	5e-05
Solid Properties	Thermal expansion coefficient	1E-06 (K^{-1})	1.80E-04
	Specific heat	1000 ($J \cdot kg^{-1} \cdot K^{-1}$)	–
	Compressibility	2E-10 (Pa^{-1})	9.82E-03
	Density	2650 ($kg \cdot m^{-3}$)	2.5
	Porosity	0.01	0.01
	Thermal conductivity (A)	2 ($W \cdot m \cdot K$)	–
	Thermal conductivity (B)	2 ($W \cdot m \cdot K$)	–
	Thermal conductivity (C)	6 ($W \cdot m \cdot K$)	–

Table 1: Table of parameters used for the best fitting temperature profile, matching that of GPK2 (see Figure 4.

At this depth, it is acknowledged that bottom boundary conditions are extremely complex and characterised by contrasting mineral assemblages and fracture clusters. However, the primary focus is on the characteristics of the fracture zone located at 3492m depth and its influence on the convection processes above this depth, therefore a bottom temperature boundary condition inferred from the bottom hole temperature of GPK2 (Figure 2) is adequate. Material properties are chosen based on previous modelling studies (e.g. Le Carlier et al., 1994; Bächler et al., 2003; Magnenet et al., 2014), where permeability and thermal conductivity values are averaged over each rock type. Table 1 details the parameters used in this study.

This study follows the approach of Vidal et al. (2015), who showed that such parameterised models are well suited to understand the driving phenomena at play. This prominent fracture zone at 3492m depth has been identified to have a thickness of 8m (Dezayes et al., 2010). No direct permeabilities have been derived for this fracture zone, but an equivalent porous medium (EPM) permeability was obtained from spinner log analyses, performed in the open hole section containing this fault Evans et al. (2005). The EPM permeability of this section was $3\times10^{-16}m^2$, and decreased to $1.5\times10^{-17}m^2$ when the fault was excluded from hydraulic testing. Spinner logs indicate that almost all of the flow occurred at this fracture zone, therefore in this study, an end-member upper limit scenario is assumed where all the flow is entirely governed by this fault at 3492m. Following this, the permeability of this zone can be inferred from the difference between the inclusion and exclusion tests Evans et al. (2005), where the value of $2.85\times10^{-16}m^2$ can be taken as a reasonable estimate for this fracture zone.

3.2 Mesh Sensitivity Analysis

In order to trust the simulation results, a mesh sensitivity analysis for the geometry described (Figure 3) is performed beforehand in order to determine the number of elements in the mesh that should be used in this study. Of particular interest are the fluid and heat flow processes within the fault, pointing to the necessity to sufficiently characterise this feature. For this sensitivity analysis, mesh geometry and values of material properties are kept constant while the number of elements in the mesh are varied, with extra focus on the fault. In this model, the temperature profile of GPK2 is used to quantify numerical convergence. Steady state temperature results varying the number of mesh elements are plotted against GPK2 data and numerical convergence is observed for approximately 11,000 elements. To ensure reliable results, 15,000 elements are used for all simulations.

4. RESULTS

This section presents the results of this study, first by matching the temperature profile of GPK2 using the traditional hydrothermal convection equations.

4.1 TH Model

In this fundamental analysis, the aim is to reconcile the permeabilities of the fracture zone used in previous studies ($1\times10^{-14}m^2$) to the inferred realistic value of $2.85\times10^{-16}m^2$ (Evans et al., 2005), whilst fitting the temperature profile of GPK2 as closely as possible. An average value of the order of $10^{-15}m^2$ is chosen as an initial attempt. In this scenario, temperature boundary conditions at the top and bottom of the model are imposed from GPK2 data, and a minimum width of 370m is derived by trial and error to sustain the (red) temperature profile obtained in Figure 4. With these conditions, the temperature profile obtained sufficiently matches that of GPK2. Given the inverse relationship between fault width and permeability, the unrealistically large value of 370m was expected. Bächler et al. (2003) used a higher value for permeability, but still obtained a fault width of 200m. Clearly, some inconsistencies remain between the observations and the numerical models used to model hydrothermal convection.

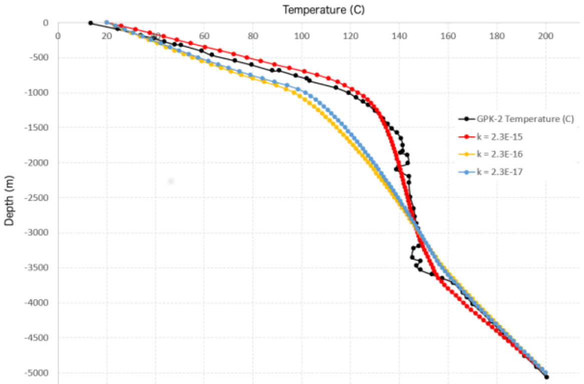

Figure 4: Simulated temperature profiles varying fault widths and permeabilities. GPK2 temperature profile is displayed in black.

Recent information of fracture aperture and thickness show that some of the model assumptions are not in agreement with the observed values. Firstly, fracture zone thickness derived from borehole images in Soultz have been averaged to be approximately 12m (Dezayes et al., 2010). Genter et al. (2000) illustrates a conceptual lithofacies of the granite, spanning approximately 10m in width, consisting of a quartz-filled fault core surrounded by cataclased brecciated granite. Particularly for the fracture zone at 3492m depth, the thickness is found to be 8m (Dezayes et al., 2010). This value is a stark contrast to the 370m fault width used in the numerical model, which should therefore be reduced considerably. This would naturally require using higher permeabilities to compensate and still match the observed temperature profile. However, the permeabilities used for the model are also relatively high ($2.30\times10^{-15}m^2$), and already fall outside the natural permeability estimated ($2.85\times10^{-16}m^2$) by one order of magnitude, even in the end-member scenario.

Another limitation to this approach is that the best fit for the temperature profile was obtained by directly plotting the temperature in the centre of the fault. This strongly idealised scenario remains an end-member case where the large vertical temperature gradient should be easily matched for realistic values of geometry and material properties. Realistic evidence suggests there is no 'single' fault zone, instead small fracture zones are interconnected to each other in small distances (e.g. Ledésert et al., 1993; Dezayes et al., 2010; Ledésert et al., 2010). Smaller widths however, will result in the localisation of fluid flow to thinner pathways. This decreased interaction with the rock mass/host rock will require higher temperatures and faster velocities to produce the same effect.

To address these issues, the permeabilities required to produce the same temperature for decreasing fault widths are examined. The following section discusses the implementation and results of the analysis.

4.2 Fault Width and Permeability Analysis

As an initial study, the fault width of 370m is maintained whilst decreasing permeability to observe its effect on the temperature profile. Figure 4 displays the temperature profiles taken at the core of the fault for decreasing permeability. The best fitting temperature profile is the one presented in Section 4.1, obtained with a permeability of the order of $10^{-15}m^2$. Although the temperature boundary conditions are fixed at the top and bottom of the model, the behaviour of the temperature profile significantly deteriorates with decreasing permeability, especially at depths between

1km and 3.5km. In these profiles, the gradient eventually diffuses to the standard geothermal gradient of approximately 30ºC/km, matching that of the lower branch.

The permeability of the fracture at 3492m depth is approximated to be around the order of 10^{-16}m^2, inferred in Section 4.1. Using this value, the temperature profile matches the lower branch but falls short of the profile obtained from GPK2 by almost 20ºC in other parts (see Figure 4). We then present an investigation of the permeabilities required for decreasing fault widths, with the consideration of only thermal and hydraulic (TH) processes.

To perform such an analysis, a zone of 'diffuse permeability' is first defined around the fault zone to match geological observations of damage zones around faults (e.g. Mitchell et al., 2011). This is represented using a bell-curve profile within the fault, where the largest value of permeability is in the centre and values gradually diffuse into the background value of the host rock. This portrayal of permeability allows the narrowing of fault widths without excessively refining the mesh, as well as accounting for the damage zone and/or hydrothermally altered permeabilities, following Mitchell et al. (2011) and Genter et al. (2000).

To obtain such a permeability profile, normalised permeability boundary conditions are first assigned to the background (k = 0) and centre of the fault (k = 1), outlined in red in Figure 3. The diffusion equation is then solved for the permeability variable over a transient simulation, where a fixed value of permeability is imposed as a boundary condition at the centre of the bell-curve, as detailed in (Tung, 2018). The desired width can then be extracted by hand-picking a given timestep, and be read as an initial solution for a transient simulation. Values of permeability can be computed by using the permeabilities assigned to the fault and basement:

$$k_{real} = \frac{k_{fault} - k_{basement}}{\alpha}$$

where k is the permeability and α the constant of the Lewis number,

$$\alpha = \frac{\mu_{f_0}\, c_{th}\, \beta_m^*}{\sigma_{ref}}$$

Note that all symbols and the Lewis number approach are detailed in (Tung, 2018). Single simulations are then run for each value of maximum permeability assigned to the centre of the fault. The methodology described allows the definition of a fracture zone with varying permeability (using a bell-shaped distribution) over any desired total width. The value of the maximum permeability at the centre of that fracture zone can then be selected independently.

This process is used to determine the total width W required for a given value of maximum permeability (kc assigned to the centre) to match the temperature profile at GPK2, where W is taken as two standard deviations of the bell curve. In this analysis, three data points are obtained. For decreasing values of W from 370m, 309m and 275m, the permeability kc is found to increase from 2×10^{-15}m^2 to 8×10^{-15}m^2 and 2×10^{-14}m^2 respectively (see Table 2). The high value of permeability for W=275m points to the futility of continuing this matching exercise for narrower values of W.

Table of Averaged Mechanical Values			
	Values Used in This Study	Documented Values	References
Frictional Coefficient	0.5	0.10 - 0.64	Plenefisch and Bonjer (1997)
Angle of Fault (°)	63	63	Dezayes et al. (2010)
Slip Rates ($mm \cdot yr^{-1}$)	0.5	0.1 - 0.7	Ahorner (1975), Buchmann and Connolly (2007)

Table 2: Table of mechanical parameters used to calculate values for Gr. Values used in this study are representative and an averaged from those documented in literature.

From this analysis, it can be seen that unrealistically high permeabilities are obtained for widths below 100m, which exceeds the derived value of the order 10^{-16}m^2 by several orders of magnitude.

Therefore, the question remains unanswered: how is it possible to match the current temperature profile of GPK2 with a fracture zone of 8m, especially if the permeability of best case scenario is inferred permeability is at best in the order of 10^{-16}m^2. The consideration of purely TH-processes is insufficient to explain such a phenomenon and obviously points to the presence of other physical processes that have been so far neglected. The next step in this study is to consider mechanical deformation through the presence of creeping faults.

4.3 THM Model

Soultz is located in an active graben setting (Evans et al., 2005) and subsidence and slip rates of the Rhine Graben have been calculated to be in the order of 0.1mm/yr to a maximum of 0.5mm/yr, with observed rates between 0.2mm/yr − 0.7mm/yr (Ahorner, 1975; Buchmann and Connolly, 2007). Well log data also identifies clusters of cataclastic shear structures around fracture zones in the reservoir (Evans, 2005). Following the study of Tung et al. (2017), it was observed that the steady creep of active faults could trigger convection at lower permeabilities. This section investigates the effect of heat generated from realistic slip rate velocities and its effect on the overall convection behaviour in the model.

The amount of heat generated by friction within the fault and not absorbed by the system is expressed using the Gruntfest number (Gr) – see (Tung et al., 2017). Following the assumptions for a fault experiencing steady creep, realistic slip rates can be expressed using Gr values.

For this model, a reference slip rate of 10^{-16}s^{-1} is assumed, calculated from the averaged slip velocities (Ahorner, 1975) and lithospheric thickness (Geissler et al., 2010). Values for fault shear stress were calculated from averaged literature values (see Table 6.3), resulting in τ_n = 76.26MPa. The yield stress can be determined using $\tau_y = C_0 + \mu(\tau_n - P_0)$, where C_0 is the cohesive strength, μ the frictional coefficient, and P_0 the pore pressure. Following the assumptions of (Plenefisch and Bonjer, 1997), the cohesive strength is assumed to be zero, thereby obtaining τ_y=45.75MPa. From these parameters, a Gruntfest number of Gr = 6.84×10^{-10} is determined for averaged values documented in literature (Tung et al, 2017).

Simulations using realistic values of Gr show no perceptible improvement to the temperature profile of GPK2. Only excessive values, increased by four orders of magnitude, start affecting the results in a perceptible manner. Attempts were made to run narrower widths, higher permeabilities and higher Gruntfest numbers, but could not match the temperature profile adequately with realistic values of material properties. This however, is not the focus of the study as the goal is to investigate and identify the key parameters of the driving processes in a system.

From this analysis of THM processes, it is apparent that shear heating is not the main driver characterising the heat and fluid flow processes in the reservoir. Rather, more complex processes are at play and the next step would be to consider chemical processes. It has been observed indeed that chemistry plays an influential role in these settings, as hydrothermally altered zones are most prevalently found in and around fault zones (Ledésert et al., 1999; Schleicher et al., 2006; Ledésert et al., 2010).

5. DISCUSSION AND CONCLUSION

The aim of this study is to identify the driving parameters of the fracture zone at approximately 3500m depth. The exclusive simulation of TH processes in the reservoir was insufficient to adequately characterise the heat and fluid flow observations. It was observed that unrealistic high permeabilities were required for sustaining convection in the reservoir when realistic fault widths were considered (see Table 6.2). Mechanical deformation was then included into the model, expressed by steadily creeping faults. Using values of slip rates documented in literature, the temperature profile was marginally improved but still failed to match the well data, differing by 20ºC particularly in the up-flow of fluid in the sub-vertical fault network. This study affirms the lack of physics represented by purely THM processes, and indicates the need of a THMC approach to describe such complex geothermal settings.

5.1 Evidence of Hydrothermal Alterations

Thorough analysis of macroscopic fractures at Soultz-sous-Forêts suggests that the granitic basement has experienced three hydrothermal alteration events (Genter and Traineau, 1996). Of particular interest is the alteration sequence which produced localised fractures. These organised clusters of fractures collectively characterises a structural trend which is evidence of extensive shear and have also been reactivated since the Tertiary (Dezayes et al., 1995; Genter et al., 1996). Controlled by such dynamic tectonism, these extensive fractured clusters have been identified as the main pathways through which fluid flows and circulation in the granitic basement is promoted (Kohl et al., 1995; Lampe and Person, 2000; Evans, 2005).

Major pathways of fluid flow in the Soultz reservoir have been identified to be through hydrothermally altered granite, localised around fracture zones. (Dezayes et al., 1995; Genter et al., 1996; Ledésert et al., 1999; Schleicher et al., 2006). Fluid circulation in these fracture zones have resulted in strong dissolution of primary minerals and precipitation/deposition of some altered minerals (Genter et al., 2010). Surprisingly, the most efficient fractures are characterised by a wide halo of alteration on either side of the fracture, even though poor connectivity exists between such fractures (Ledésert et al., 1993). The core of these fractures has been found to be filled with various hydrothermal minerals, consisting predominantly quartz, carbonates, clay minerals, and chlorite (Genter and Traineau, 1996).

5.2 Towards a THMC-Coupled Approach

The identification of key parameters which govern the chemical processes in a tightly coupled system can be challenging. Lampe and Person (2000) suggest a fully-coupled THMC system where frequent reactivation of faults assists fluid flow, while the episodic mineralisation along and within faults obstructs flow through the reservoir. This concept is further investigated in this section. The use of a stability analysis such as the pseudo-arclength continuation method used by Tung et al. (2017) can help determine the critical value of key parameters once they are identified.

Shear heating and pore fluid pressurisation have been documented to be primary mechanisms resulting in fault slip (e.g. Garagash and Rudnicki, 2003; Rice, 2006). Following this, in addition to the THM processes considered so far in this study, the idea of a mechanical-chemical oscillator (Alevizos et al., 2014) is proposed for the chemical process governing the fracture zone at 3492m. In this model, a fluid-saturated, steadily creeping fault under shear experiences fluid-release reactions triggered by the shear heating generated from the creep. The theoretical conditions which govern this model are the dehydration of minerals and an endothermic chemical reaction, which could be found in realistic conditions at Soultz. At Soultz, strong dissolution and precipitation of minerals have indeed been found around fracture zones. Specifically, the fracture zone at 3492m depth contains precipitated clays and has been found to have experienced shear deformation, from the presence of illite and the evidence of cataclastic fragments, respectively (Genter and Traineau, 1996; Evans, 2005). Many geochemical studies have been performed to investigate the main chemical reactions occurring, and in particular the reaction K-feldspar + Al-clays → illite + quartz has been previously indicated as predominant in this particular fracture zone (Ledésert et al., 1999) in order to apply this oscillatory model. The presence of illite can be expected to contribute to lowering the frictional coefficient of the fault, which could cause more slip on the fracture zone, suggesting an evidence of the chemo-mechanical oscillator.

The model in (Alevizos et al., 2014) describes a system where the fault movement and chemical reactions can occur repeatedly due to the chemical and thermal feedback loops. From the evidence of cataclastic sheared features, episodic fault reactivation is proposed for the fracture zone located at 3492m depth. In such a model, the fault is stationary for most of the time which results in ambient low permeability. During its reactivation however, permeability can temporarily increase by several orders of magnitude, and fluid is driven through the fault. The presence of illite suggests a dissolution/precipitation reaction where illite enhances slip, until the endothermic reaction absorbs more heat than shear heating produces and the fault enters a stationary regime. Such chemo-mechanical oscillators have been demonstrated so far in deep, tectonically active environments (e.g. subduction zones), and no comprehensive study has been performed yet in such shallow environments. As such, the investigation of this fault in Soultz could be challenging as the environment is too shallow for the phenomenon to be confidently identified, and would have a subtle signature, should it be present. Although the use of a numerical stability analysis can assist to identify the key driving processes, the full study of such chemical processes is extremely complex and hence lies outside the scope of this paper, but is proposed as future work. This study could be extended to simulating and evaluating the behaviour of the vertical fault network, to investigate if the temperature profile obtained from GPK2 is reproducible with a fully coupled THMC modelling approach. Such studies could greatly contribute to the understanding of a time-dependent permeability structure of the processes occurring at Soultz.

ACKNOWLEDGEMENTS

This paper stems from unpublished work of Rebecca Tung's PhD in collaboration with the Karlsruhe Institute of Technology. The work was supported by the Australian Research Council (ARC DP170104550, DP170104557) and the strategic SPF01 fund of UNSW, Sydney. R. Tung was supported by the Australian Government Research Training Program Scholarship and acknowledges support from the Australian Technology Network's Industry Doctoral Training Centre (ATN-IDTC Scholarship).

REFERENCES

Ahorner, L. Present-day stress field and seismotectonic block movements along major fault zones in central Europe. Tectonophysics 29 (1-4), 233–249. (1975)

Alevizos, S., Poulet, T., Veveakis, E. Thermo-poro-mechanics of chemically active creeping faults. 1: Theory and steady state considerations. Journal of Geophysical Research: Solid Earth 119 (6), 4558–4582. (2014)

Bächler, D., Kohl, T., Rybach, L. Impact of graben-parallel faults on hydrothermal convection–Rhine graben case study. Physics and Chemistry of the Earth, Parts A/B/C 28 (9), 431–441. (2003)

Baillieux, P., Schill, E., Abdelfettah, Y., Dezayes, C. Possible natural fluid pathways from gravity pseudo-tomography in the geothermal fields of northern Alsace (upper Rhine graben). Geothermal Energy 2 (1), 16. (2014)

Benderitter, Y., Elsass, P. Structural control of deep fluid circulation at the Soultz HDR site, France: a review. In: International Journal of Rock Mechanics and Mining Sciences and Geomechanics Abstracts. Vol. 3. p. 104A. (1996)

Bergerat, F. Stress fields in the European platform at the time of Africa-Eurasia collision. Tectonics 6 (2), 99–132. (1987)

Buchmann, T. J., Connolly, P. T. Contemporary kinematics of the upper rhine graben: a 3D finite element approach. Global and Planetary Change 58 (1-4), 287– 309. (2007)

Clauser, C., Villinger, H. Analysis of conductive and convective heat transfer in a sedimentary basin, demonstrated for the Rheingraben. Geophysical Journal International 100 (3), 393–414. (1990)

Dezayes, C., Genter, A., Gentier, S. Fracture network of the EGS geothermal reservoir at Soultz-sous-Forêts (Rhine graben, France). Geotherm. Resour. Council Trans 28, 213–218. (2004)

Dezayes, C., Genter, A., Valley, B. Structure of the low permeable naturally fractured geothermal reservoir at Soultz. Comptes Rendus Geoscience 342 (7-8), 517–530. (2010)

Dezayes, C., Villemin, T., Genter, A., Traineau, H., Angelier, J. Analysis of fractures in boreholes of Hot Dry Rock project at Soultz-sous-Forêts (Rhine graben, France). Scientific Drilling 5 (1), 31–41. (1995)

Evans, K. F., Apr. Permeability creation and damage due to massive fluid injections into granite at 3.5 km at Soultz: 2. critical stress and fracture strength. J. Geophys. Res. 110 (B4), B04204. (2005)

Evans, K. F., Genter, A., Sausse, J., Apr. Permeability creation and damage due to massive fluid injections into granite at 3.5 km at Soultz: 1. borehole observations. J. Geophys. Res. 110 (B4), B04203. (2005)

Garagash, D. I., Rudnicki, J. W. Shear heating of a fluid-saturated slip-weakening dilatant fault zone 1. limiting regimes. Journal of Geophysical Research: Solid Earth 108 (B2). (2003)

Geissler, W. H., Sodoudi, F., Kind, R. Thickness of the central and eastern European lithosphere as seen by s receiver functions. Geophysical Journal International 181 (2), 604–634. (2010)

Genter, A., Evans, K., Cuenot, N., Fritsch, D., Sanjuan, B. Contribution of the exploration of deep crystalline fractured reservoir of Soultz to the knowledge of enhanced geothermal systems (EGS). Comptes Rendus Geoscience 342 (7), 502–516. (2010)

Genter, A., Traineau, H. Analysis of macroscopic fractures in granite in the HDR geothermal well EPS-1, Soultz-sous-Forêts, France. Journal of volcanology and geothermal research 72 (1-2), 121–141. (1996)

Genter, A., Traineau, H., Dezayes, C., Elsass, P., Ledsert, B., Meunier, A., Villemin, T. Fracture analysis and reservoir characterization of the granitic basement in the HDR soultz project (France). In: International journal of rock mechanics and mining sciences & geomechanics abstracts. Vol. 33. Elsevier Science, pp. 69A–69A. (1996)

Genter, A., Traineau, H., Ledsert, B., Bourgine, B., Gentier, S., May 28 - June 10 2000. Over 10 years of geological investigations within the HDR Soultz project, France. In: *Proceedings World Geothermal Congress*. Kyushu-Tohoku Japan. (2000)

Hooijkaas, G. R., Genter, A., Dezayes, C. Deep-seated geology of the granite intrusions at the Soultz EGS site based on data from 5 km-deep boreholes. Geother- mics 35 (5-6), 484–506. (2006)

Illies, J. H., Greiner, G. Rhinegraben and the alpine system. Geological Society of America Bulletin 89 (5), 770–782. (1978)

Jung, R., Willis-Richard, J., Nicholls, J., Bertozzi, A., Heinemann, B. Evaluation of hydraulic tests at Soultz-sous-Forêts, European HDR site. In: Proceedings of the world geothermal congress. Vol. 4. pp. 2671–2676. (1995)

Kohl, T., Bchler, D., Rybach, L. Steps towards a comprehensive thermo-hydraulic analysis of the HDR test site Soultz-sous-Forêts. In: Proceedings World Geothermal Congress. Kyushu-Tohoku Japan, pp. 2671–2676. (2000)

Kohl, T., Evans, K. F., Hopkirk, R. J., Jung, R., Rybach, L. Modelling of turbulent flow transients within Hot Dry Rock fracture systems: Preliminary results. Proc. World Geothermal Cong. (1995)

Lampe, C., Person, M. Episodic hydrothermal fluid flow in the upper Rhine-graben (Germany). Journal of Geochemical Exploration 69-70, 37–40. (2000)

Larroque, J. M., Laurent, P. Evolution of the stress field pattern in the south of the Rhine graben from the Eocene to the present. Tectonophysics 148 (1-2), 41–58. (1988)

Le Carlier, C., Royer, J.-J., Flores, E. L. Convective heat transfer at the Soultz-sous-Forêts geothermal site: implications for oil potential. First break 12 (11), 553–560. (1994)

Ledésert, B., Berger, G., Meunier, A., Genter, A., Bouchet, A. Diagenetic-type reactions related to hydrothermal alteration in the Soultz-sous-Forêts granite, France. European Journal of Mineralogy 11 (4), 731–741. (1999)

Ledésert, B., Dubois, J., Velde, B., Meunier, A., Genter, A., Badri, A. Geo- metrical and fractal analysis of a three-dimensional hydrothermal vein network in a fractured granite. Journal of Volcanology and Geothermal Research 56 (3), 267–280. (1993)

Ledésert, B., Hebert, R., Genter, A., Bartier, D., Clauer, N., Grall, C. Fractures, hydrothermal alterations and permeability in the Soultz enhanced geothermal system. Comptes Rendus Geoscience 342 (7-8), 607–615. (2010)

Magnenet, V., Fond, C., Genter, A., Schmittbuhl, J. Two-dimensional THM modelling of the large scale natural hydrothermal circulation at Soultz-sous-Forêts. Geothermal Energy 2 (1), 17. (2014)

Mitchell, T. M., Ben-Zion, Y., Shimamoto, T. Pulverized fault rocks and damage asymmetry along the Arima-Takatsuki tectonic line, Japan. Earth and Planetary Science Letters 308 (3), 284–297. (2011)

Plenefisch, T., Bonjer, K.-P. The stress field in the Rhine graben area inferred from earthquake focal mechanisms and estimation of frictional parameters. Tectonophysics 275 (1-3), 71–97. (1997)

Poulet, T., Paesold, M., Veveakis, M. Multi-physics modelling of fault mechanics using redback: A parallel open-source simulator for tightly coupled problems. Rock Mechanics and Rock Engineering 50 (3), 733–749. (2017)

Pribnow, D., Clauser, C. Heat and fluid flow at the Soultz Hot Dry Rock system in the rhine graben. In: World Geothermal Congress, Kyushu-Tohoku, Japan. pp. 3835–3840. (2000)

Pribnow, D., Schellschmidt, R., Jul. Thermal tracking of upper crustal fluid flow in the Rhine graben. Geophys. Res. Lett. 27 (13), 1957–1960. (2000)

Rice, J. R. Heating and weakening of faults during earthquake slip. Journal of Geophysical Research: Solid Earth 111 (B5). (2006)

Rousset, D., Bayer, R., Guillon, D., Edel, J. B. Structure of the southern Rhine graben from gravity and reflection seismic data (ecors-dekorp program). Tectonophysics 221 (2), 135–153. (1993)

Sausse, J., Dezayes, C., Dorbath, L., Genter, A., Place, J. 3D model of fracture zones at Soultz-sous-Forêts based on geological data, image logs, induced microseismicity and vertical seismic profiles. Comptes Rendus Geoscience 342 (7), 531–545. (2010)

Sausse, J., Fourar, M., Genter, A. Permeability and alteration within the Soultz granite inferred from geophysical and flow log analysis. Geothermics 35 (5-6), 544– 560. (2006)

Schleicher, A. M., Warr, L. N., Kober, B., Laverret, E., Clauer, N. Episodic mineralization of hydrothermal illite in the Soultz-sous-Forêts granite (upper rhine graben, france). Contributions to Mineralogy and Petrology 152 (3), 349–364. (2006)

Tung, R; On the Onset of Hydrothermal Convection in Porous Media in the Presence of Creeping Faults: Numerical Stability Analysis and Geological Applications. PhD thesis submitted (2018)

Tung, R; Poulet, T; Alevizos, S; Veveakis, E; Regenauer-Lieb, K, Shear heating in creeping faults changes the onset of convection, Geophysical Journal International 211 (1), 270-283 (2017)

Vidal, J., Genter, A., Chopin, F. Permeable fracture zones in the hard rocks of the geothermal reservoir at Rittershoffen, France. Journal of Geophysical Research: Solid Earth. (2017)

Vidal, J., Genter, A., Schmittbuhl, J. How do permeable fractures in the Triassic sediments of northern Alsace characterize the top of hydrothermal convective cells? evidence from Soultz geothermal boreholes (France). Geothermal Energy 3 (1), 8. (2015)

Ziegler, P. A. European Cenozoic rift system. Tectonophysics 208 (1), 91–111. (1992)